iScience, Volume *24*

Supplemental Information

Distinct T cell receptor repertoire diversity of clinically defined high-grade serous ovarian cancer treatment subgroups

Sanghoon Lee, Li Zhao, Latasha D. Little, Shannon N. Westin, Amir A. Jazarei, Nicole D. Fleming, Jianhua Zhang, P. Andrew Futreal, and Anil K. Sood

SUPPLEMENTAL FIGURES (FIGURES S1-18)

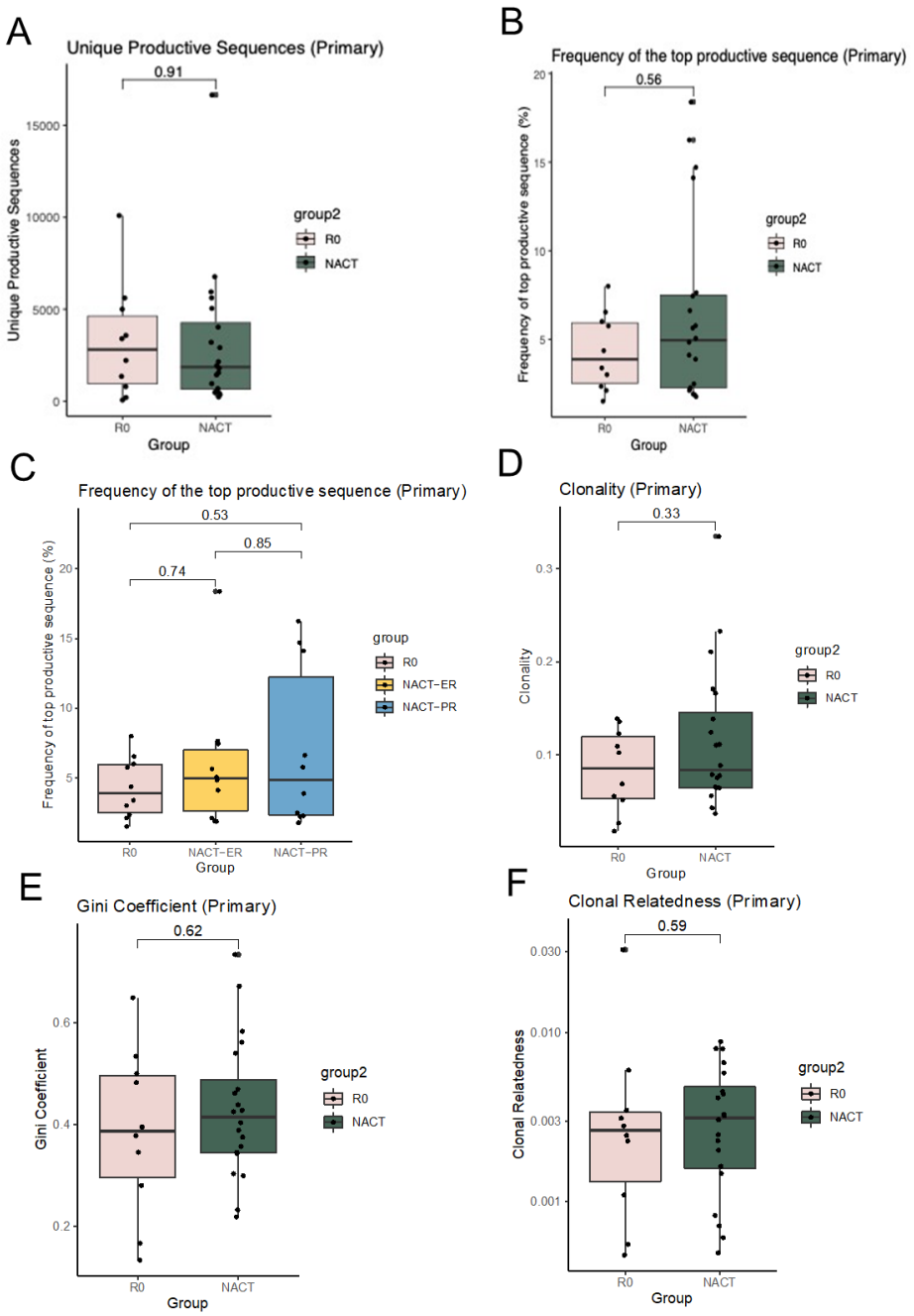

Figure S1. Comparison of T cell repertoire diversity in primary tumors across patient groups, Related to Figure 2. (**A**) Comparison of T cell repertoire richness in primary tumors between the R0 and NACT groups. TCR richness was quantified by the number of unique productive sequences. (**B**) Comparison of the frequency of the top productive sequences in primary tumors between the R0 group and NACT groups. (**C**) Comparison of the frequency of the top productive sequences in primary tumors between the NACT-ER and NACT-PR groups. (**D**) Comparison of the clonality score derived from the Shannon entropy in primary tumors between the R0 and NACT groups. (**E**) Comparison of clonal evenness derived from the Gini coefficient in primary tumors between the R0 and NACT groups. (**F**) Comparison of clonal relatedness in primary tumors between the R0 and NACT groups.

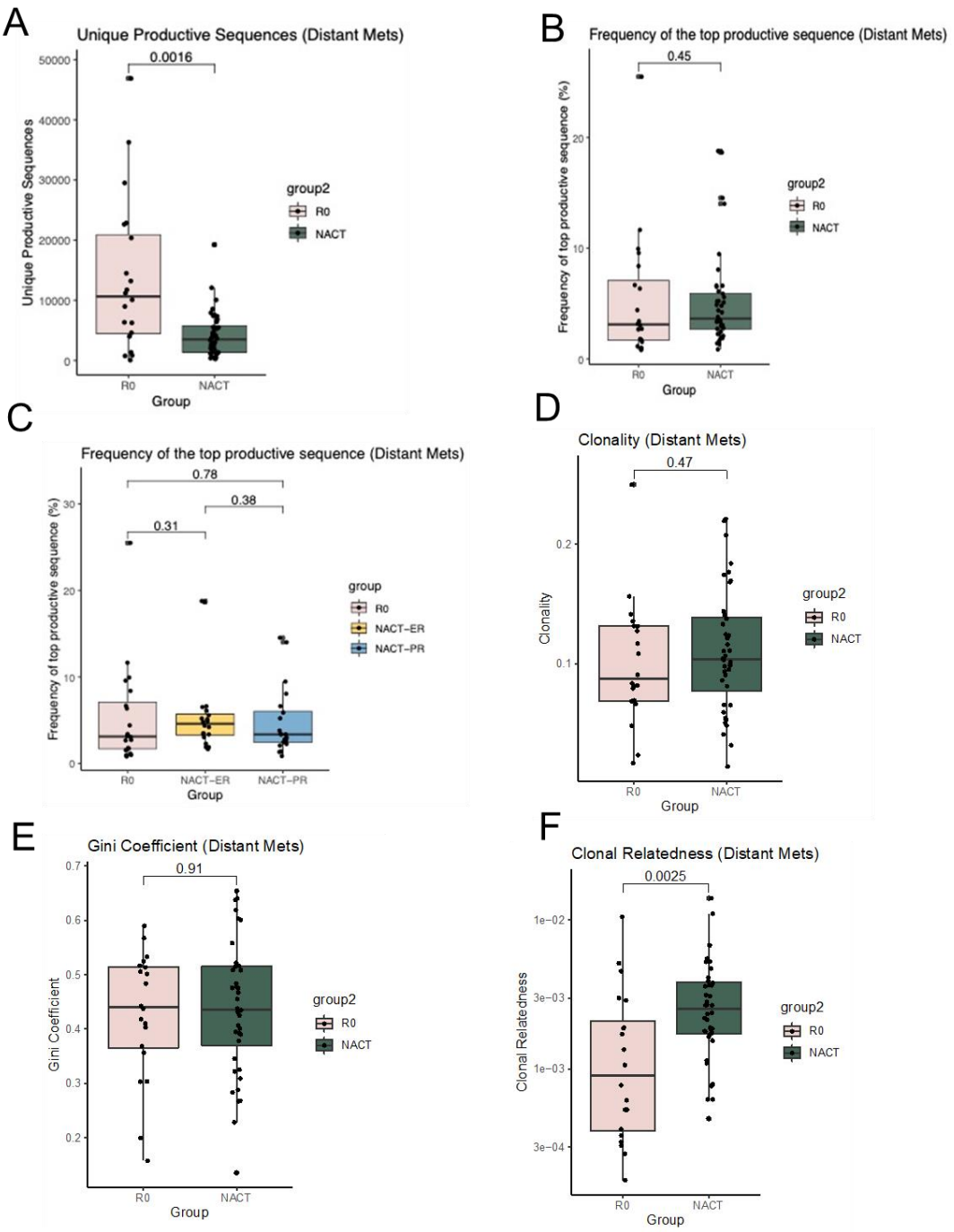

Figure S2. Comparison of T cell repertoire diversity in metastatic tumors across patient groups, Related to Figure 2. (**A**) Comparison of T cell repertoire richness in metastatic tumors between the R0 and NACT groups. TCR richness was quantified by the number of unique productive sequences. (**B**) Comparison of the frequency of the top productive sequence in metastatic tumors between the R0 and NACT groups. (**C**) Comparison of the frequency of the top productive sequence in metastatic tumors between the NACT-ER and NACT-PR groups. (**D**) Comparison of the clonality score derived from Shannon entropy in metastatic tumors between the R0 and NACT groups. (**E**) Comparison of clonal evenness derived from the Gini coefficient in metastatic tumors between the R0 and NACT groups. (**F**) Comparison of clonal relatedness in metastatic tumors between the R0 and NACT groups.

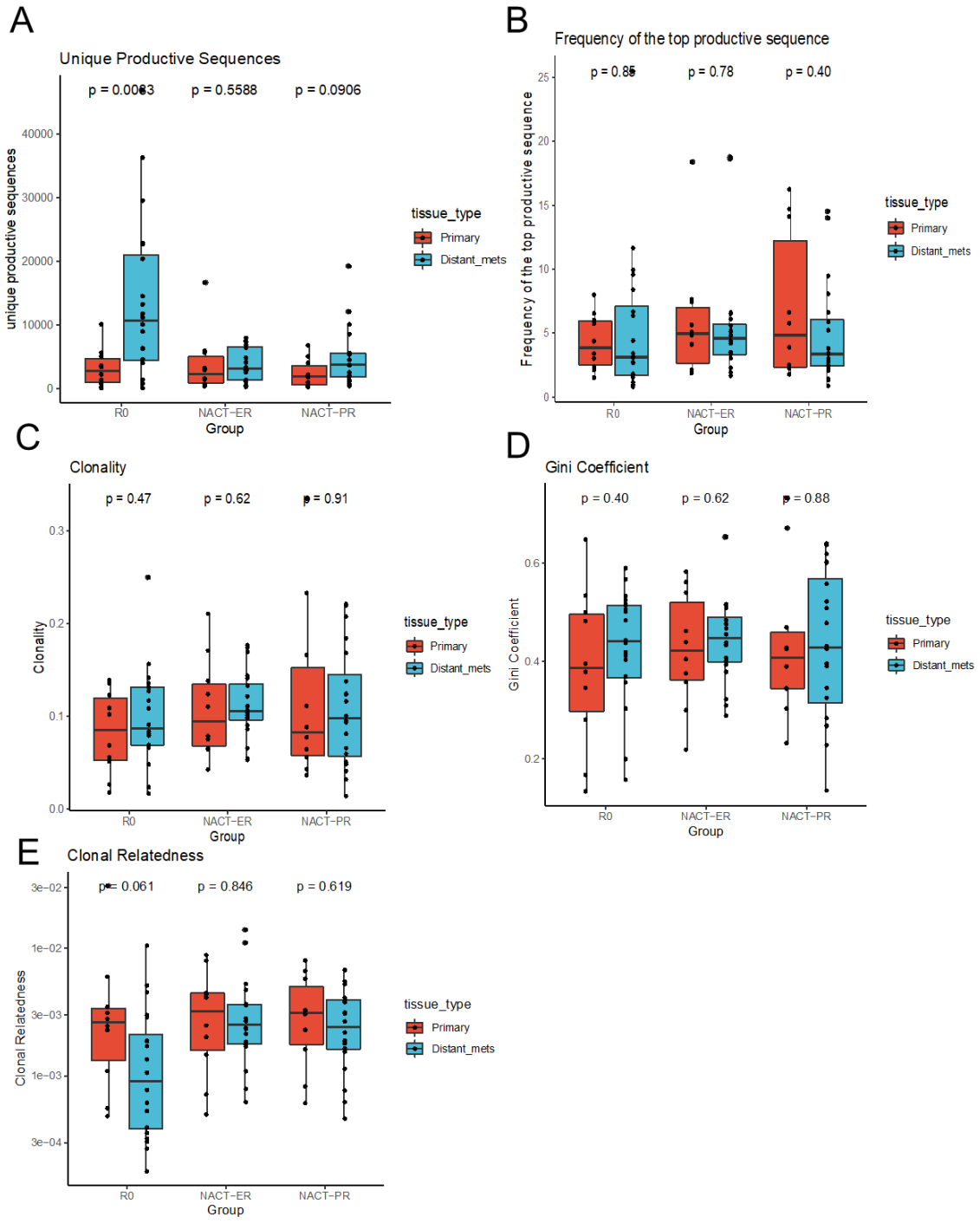

Figure S3. Comparison of T cell repertoires diversity between primary and metastatic tumors, Related to Figure 2. (**A**) Comparison of T cell repertoire richness, quantified by the number of unique productive sequences between primary and metastatic tumors. (**B**) Comparison of the frequency of the top productive sequence between primary and metastatic tumors. (**C**) Comparison of TCR clonality between primary and metastatic tumors. (**D**) Comparison of clonal evenness that was derived from the Gini coefficient between primary and metastatic tumors. (**E**) Comparison of clonal relatedness between primary and metastatic tumors.

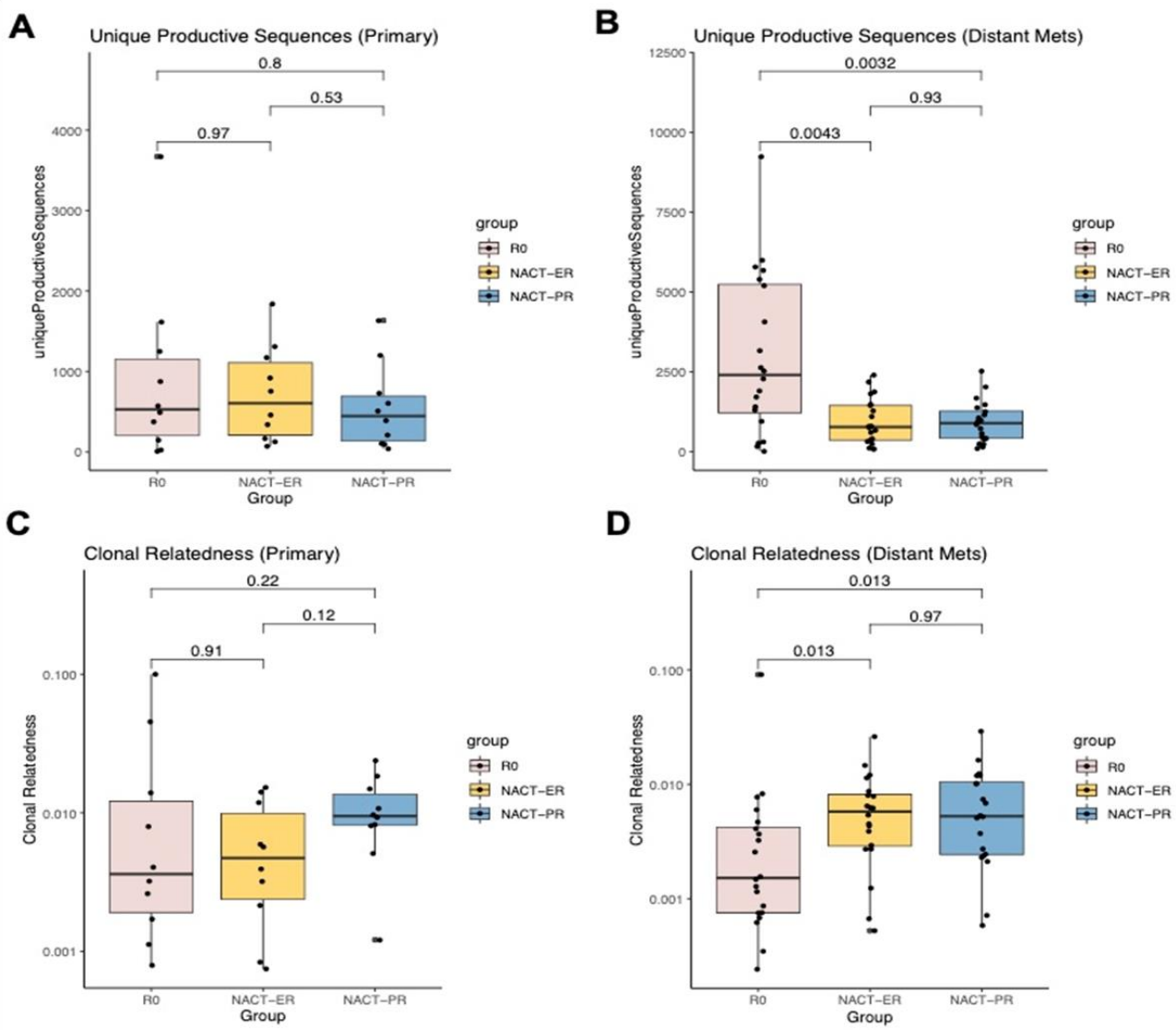

Figure S4. Diversity evaluation of T cell repertoires by the patient group after excluding TCRs with low reads count, Related to Figure 2. (**A** and **B**) Comparison of T cell repertoire richness in primary tumors (A) and metastatic tumors (B) across three groups. TCR richness was evaluated by the number of unique productive sequences, which were defined as sequences that are in frame and do not have an early stop codon. (**C** and **D**) Comparison of clonal relatedness among three groups in primary tumors (C) and metastatic tumors (D). Clonal relatedness was defined as the proportion of sequences that are related to the most frequent sequence by a defined distance threshold.

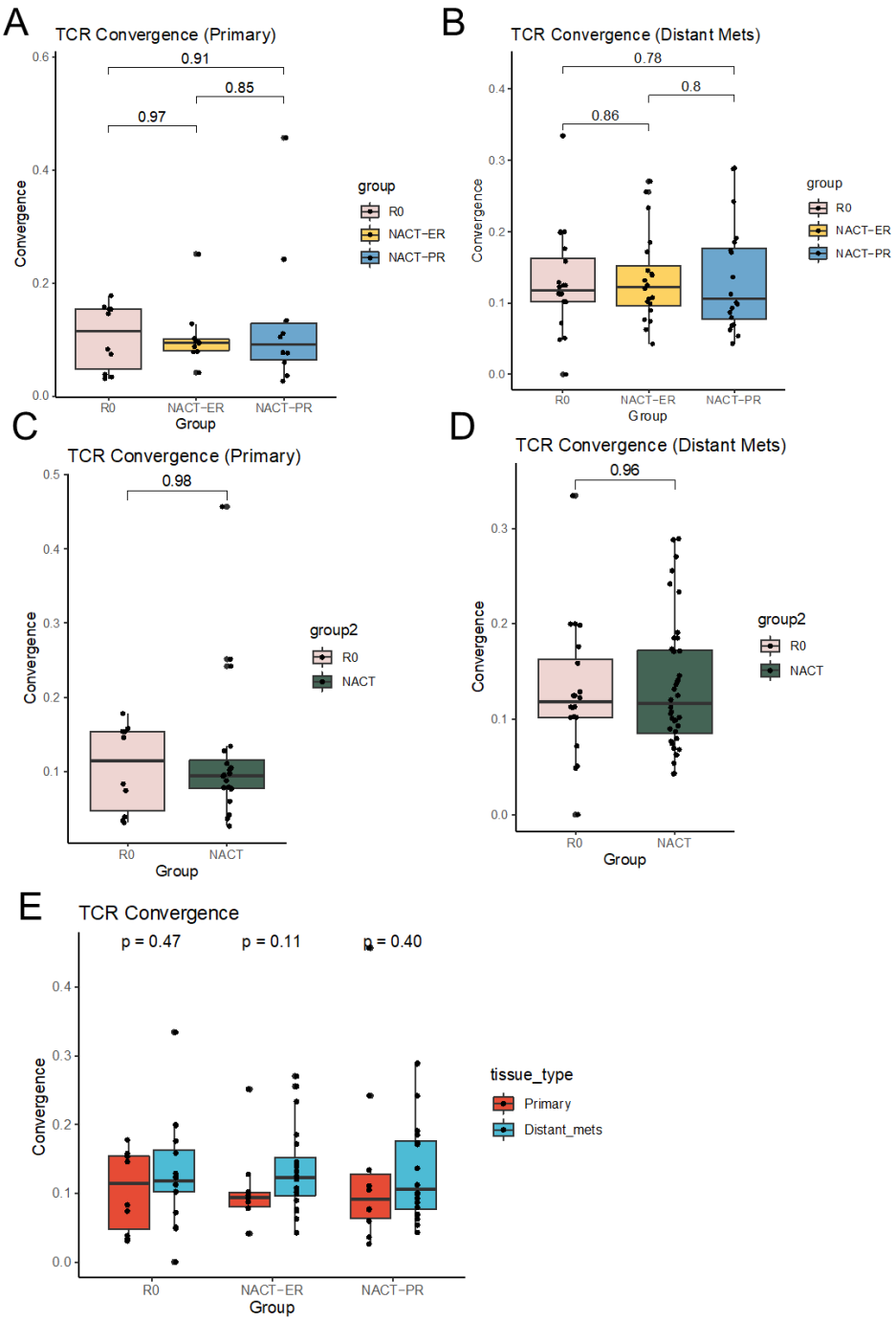

Figure S5. Comparison of TCR convergence between patient groups, Related to Figure 2. TCR convergence was calculated as the aggregate frequency of clones (unique TCRB nucleotide sequences) that share a variable gene and CDR3 amino acid sequence with at least one other identified clone. (**A, B**) TCR convergence was compared between primary tumors (A) and metastatic tumors (B) across all three groups. (**C, D**) A similar comparison was performed between the R0 and NACT groups for primary (C) and metastatic tumors (D). (**E**) TCR convergence was also compared between primary and metastatic tumors in each group.

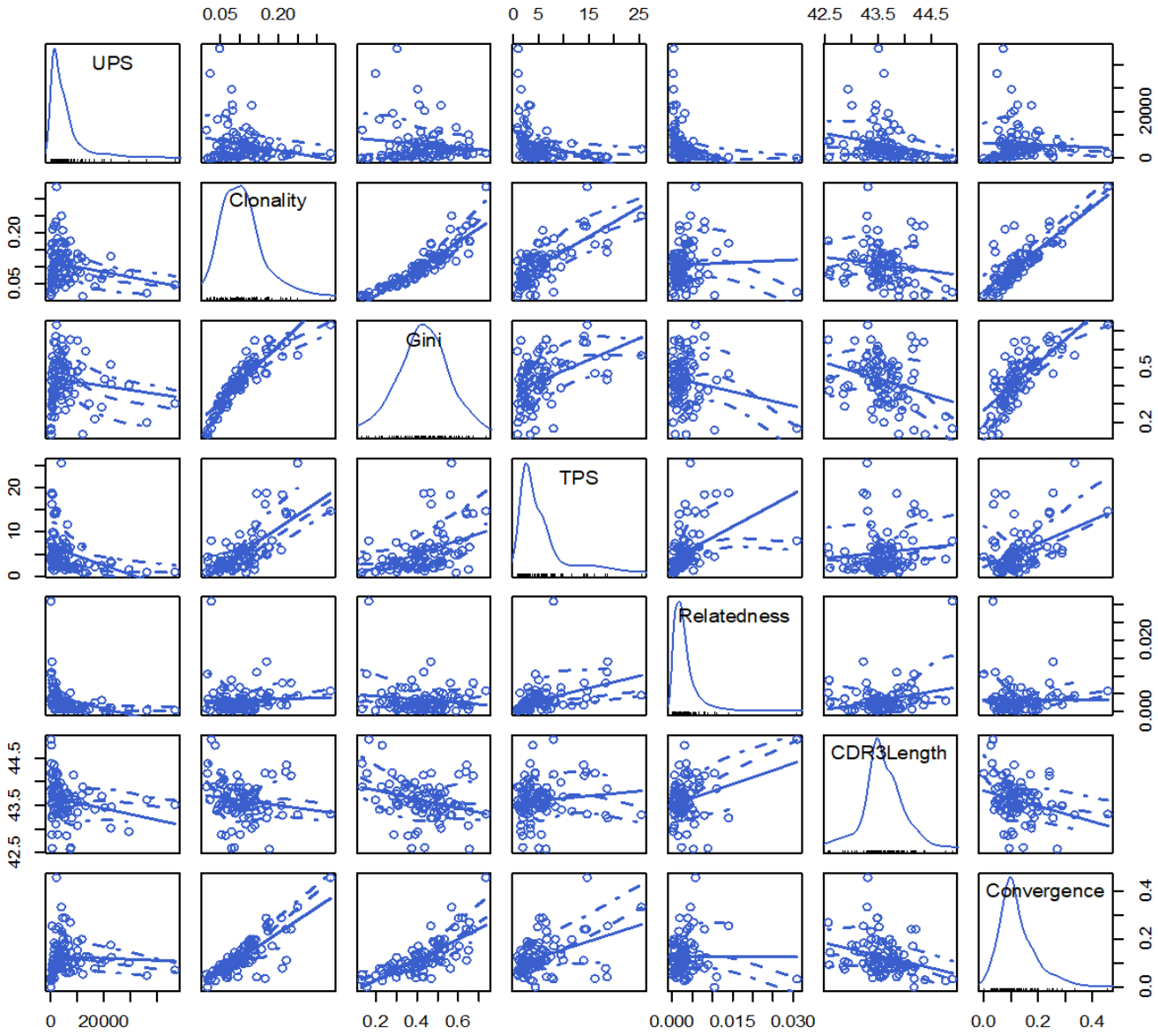

Figure S6. The matrix scatterplot of the seven metrics included in the multidimensional analysis, Related to Figure 3. The metrics include the unique productive sequences (UPS), clonality, Gini coefficient, frequency of top productive sequence (TPS), clonal relatedness, average CDR3 length, and TCR convergence. The diagonal cells show histograms of each of the variables, and each of the off-diagonal cells is a scatterplot of two metrics.

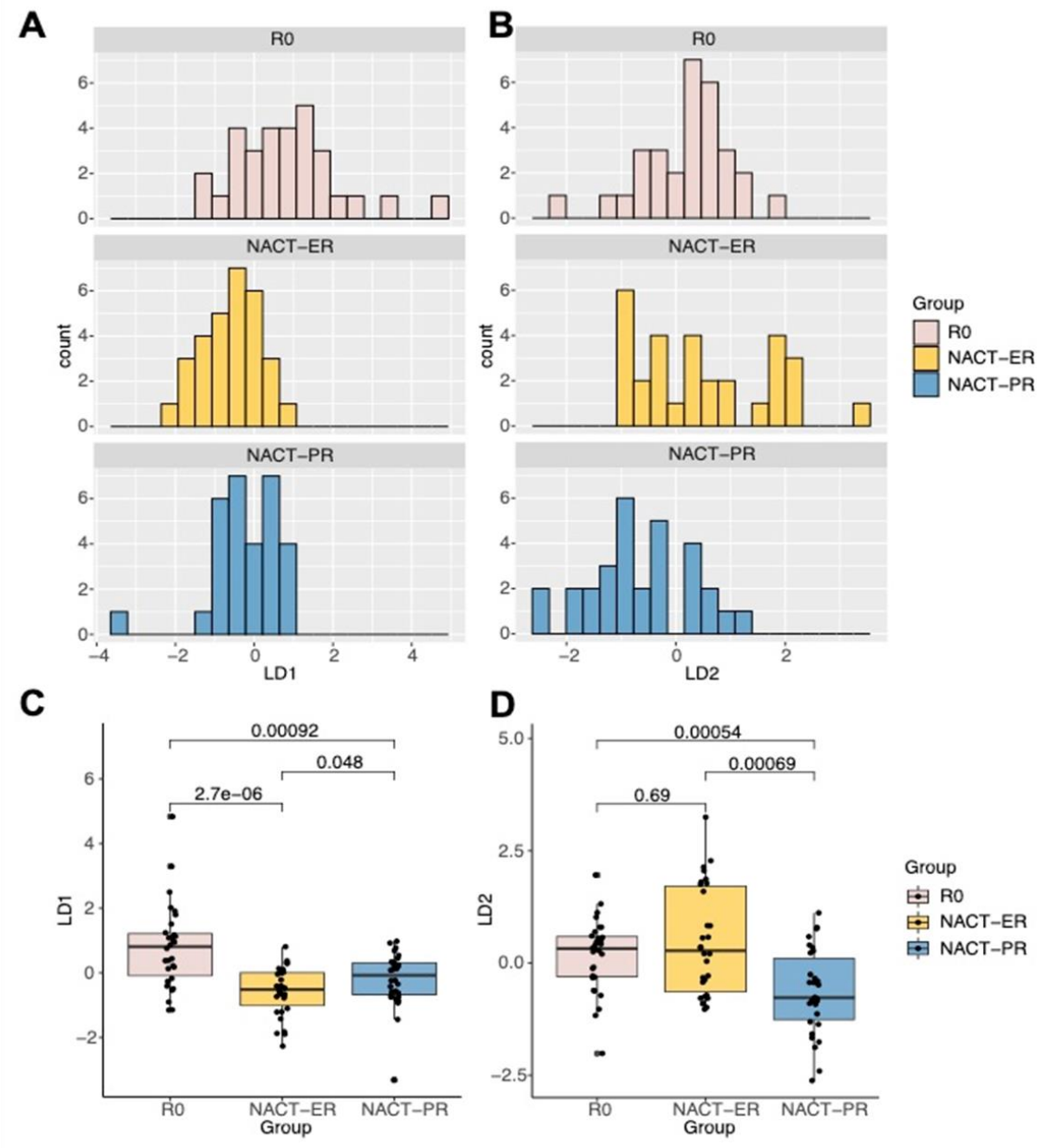

Figure S7. The results of linear discriminant analysis (LDA) , Related to Figure 3. Seven metrics were included in the analysis including unique productive sequences, clonality, Gini coefficient, frequency of top productive sequence, clonal relatedness, average CDR3 length, and TCR convergence. **A-B** show the histograms of LD1 and LD2 in three different groups and **C-D** are the boxplot of LD1 and LD2 values in three groups. Comparison between groups was performed using the Wilcoxon test.

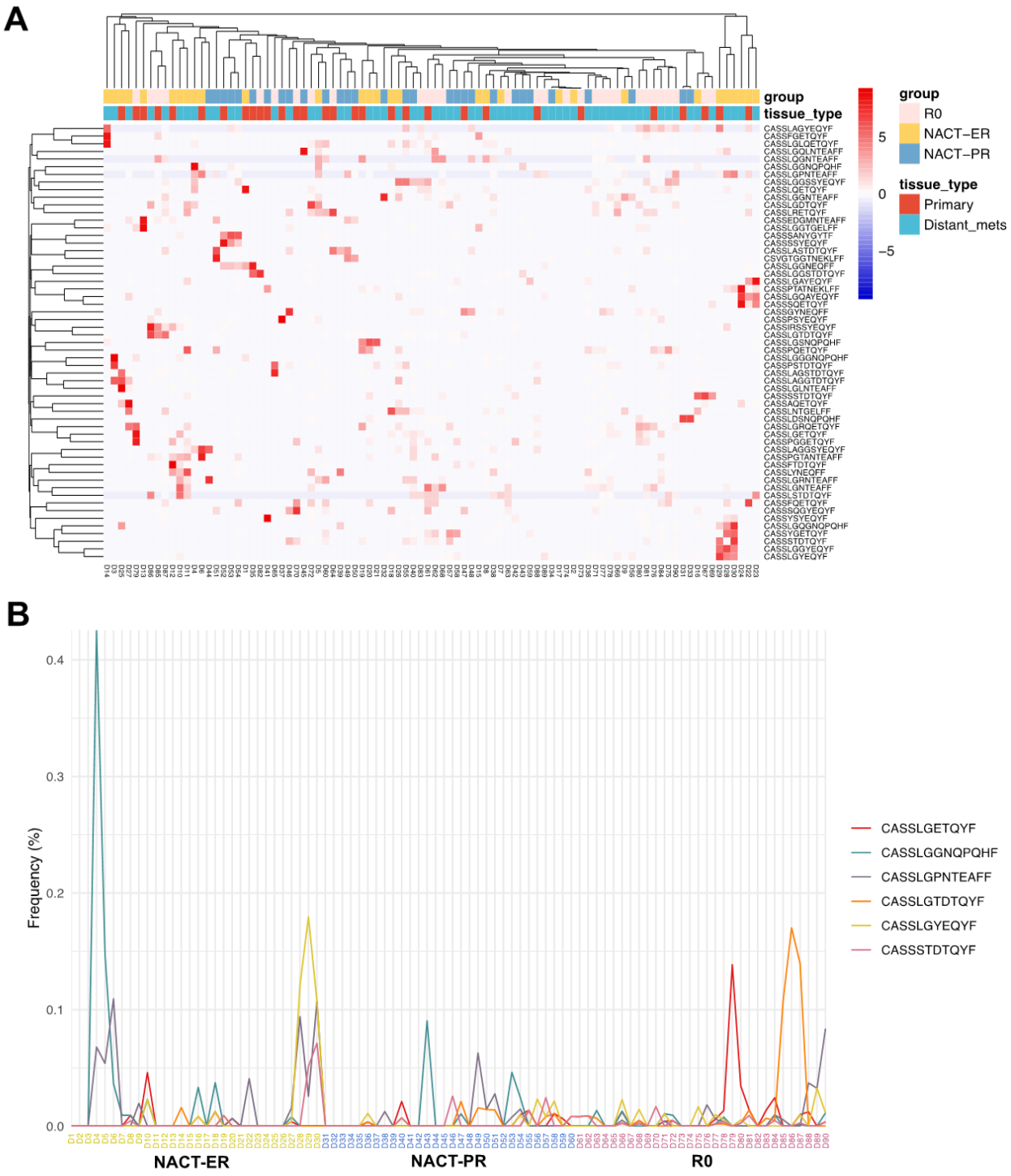

Figure S8. The dynamics of common TCRs shared by multiple samples, Related to Figure 3. (**A**) Heatmap shows the frequency of TCRs shared by at least 15% of the samples. (**B**) The trace of the most common TCRs shared by >=20 samples.

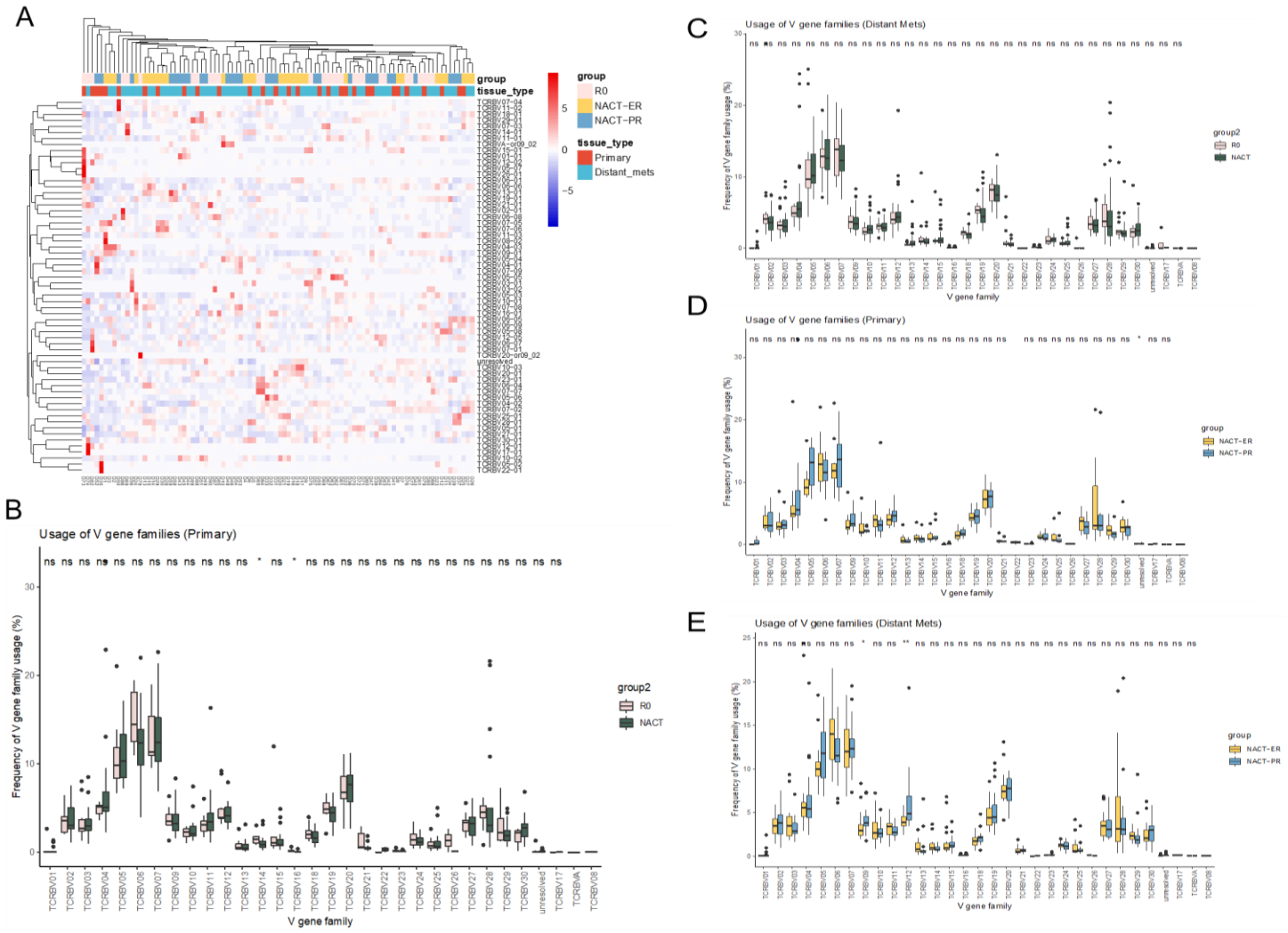

Figure S9. V gene usage in patient groups, Related to Figure 4. (**A**) Heatmap of V gene usage in all samples. (**B**) Comparison of V gene usage in primary tumors between the R0 and NACT groups. (**C**) Comparison of V gene usage in metastatic tumors between the R0 and NACT groups. (**D**) Comparison of V gene usage in primary tumors between the NACT-ER and NACT-PR groups. (**E**) Comparison of V gene usage in metastatic tumors between the NACT-ER and NACT-PR groups.

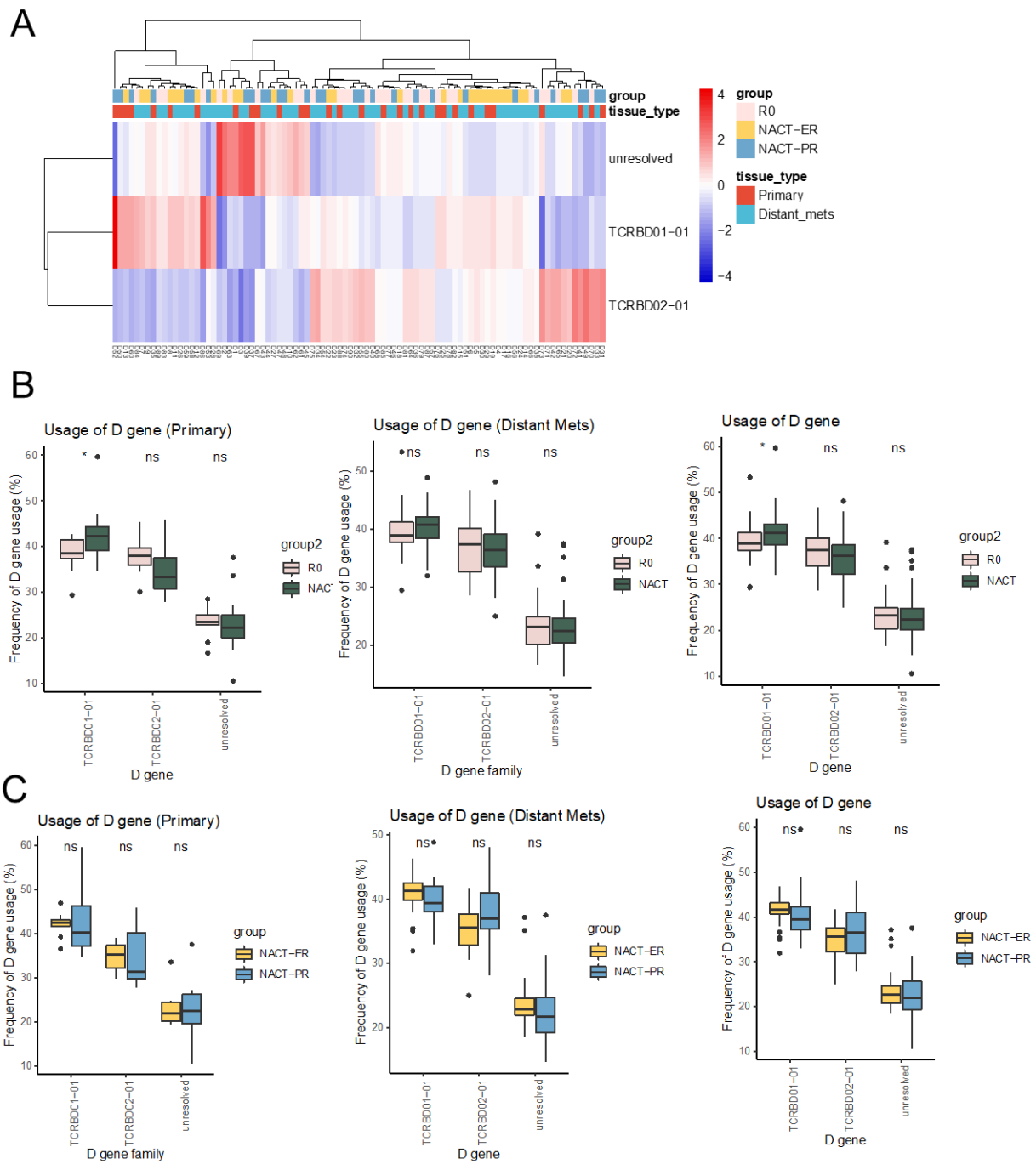

Figure S10. D gene usage in patient groups, Related to Figure 4. (**A**) Heatmap of D gene usage in all samples. (**B**) Comparison of D gene usage in primary, metastatic, and all tumors combined between the R0 and NACT groups. (**C**) Comparison of D gene usage in primary, metastatic, and all tumors combined between the NACT-ER and NACT-PR groups.

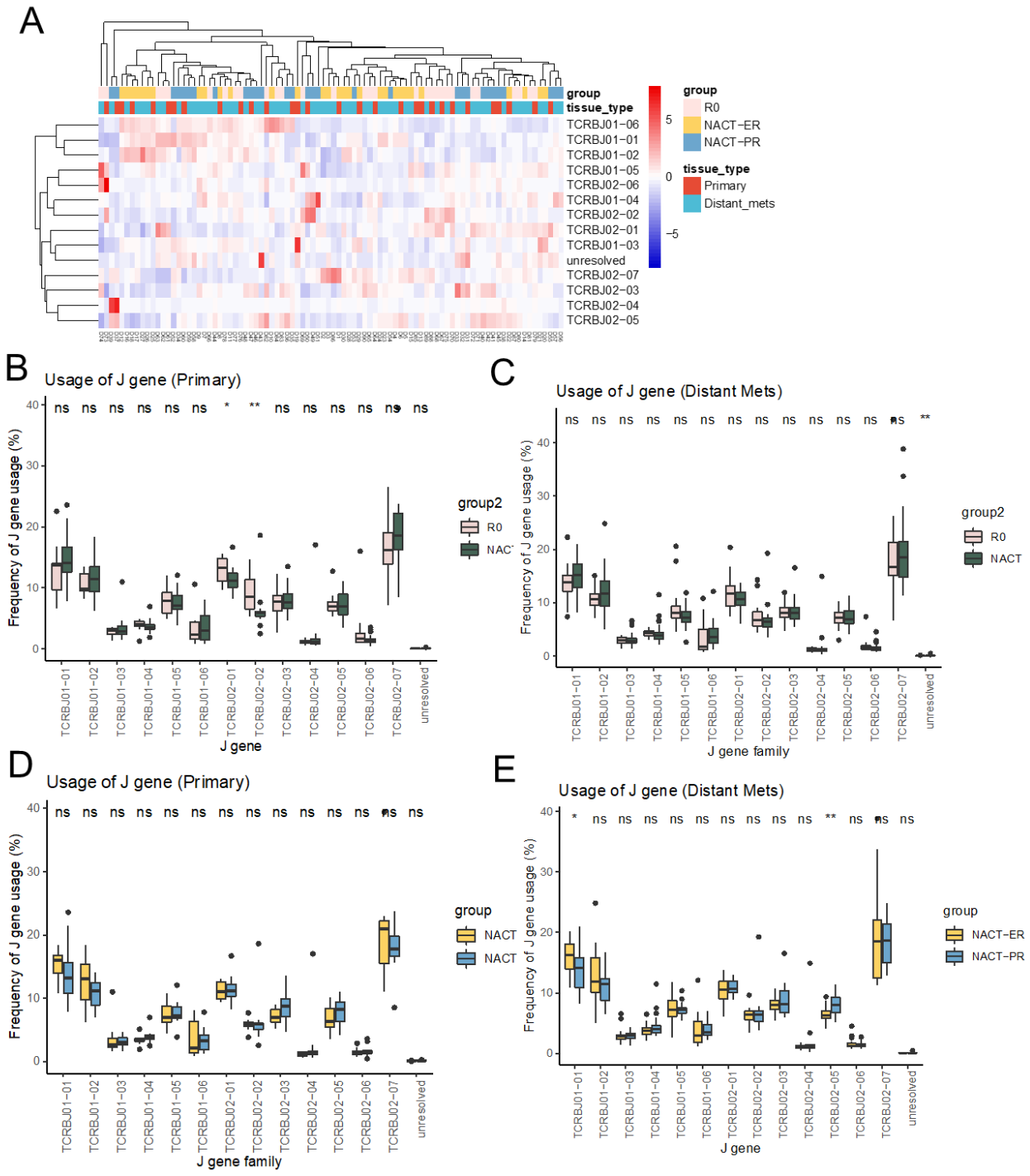

Figure S11. J gene usage in patient groups, Related to Figure 4. (**A**) Heatmap of J gene usage in all samples. (**B**) Comparison of J gene usage in primary tumors between the R0 and NACT groups. (**C**) Comparison of J gene usage in metastatic tumors between the R0 and NACT groups. (**D**) Comparison of J gene usage in primary tumors between the NACT-ER and NACT-PR groups. (**E**) Comparison of J gene usage in metastatic tumors between the NACT-ER and NACT-PR groups.

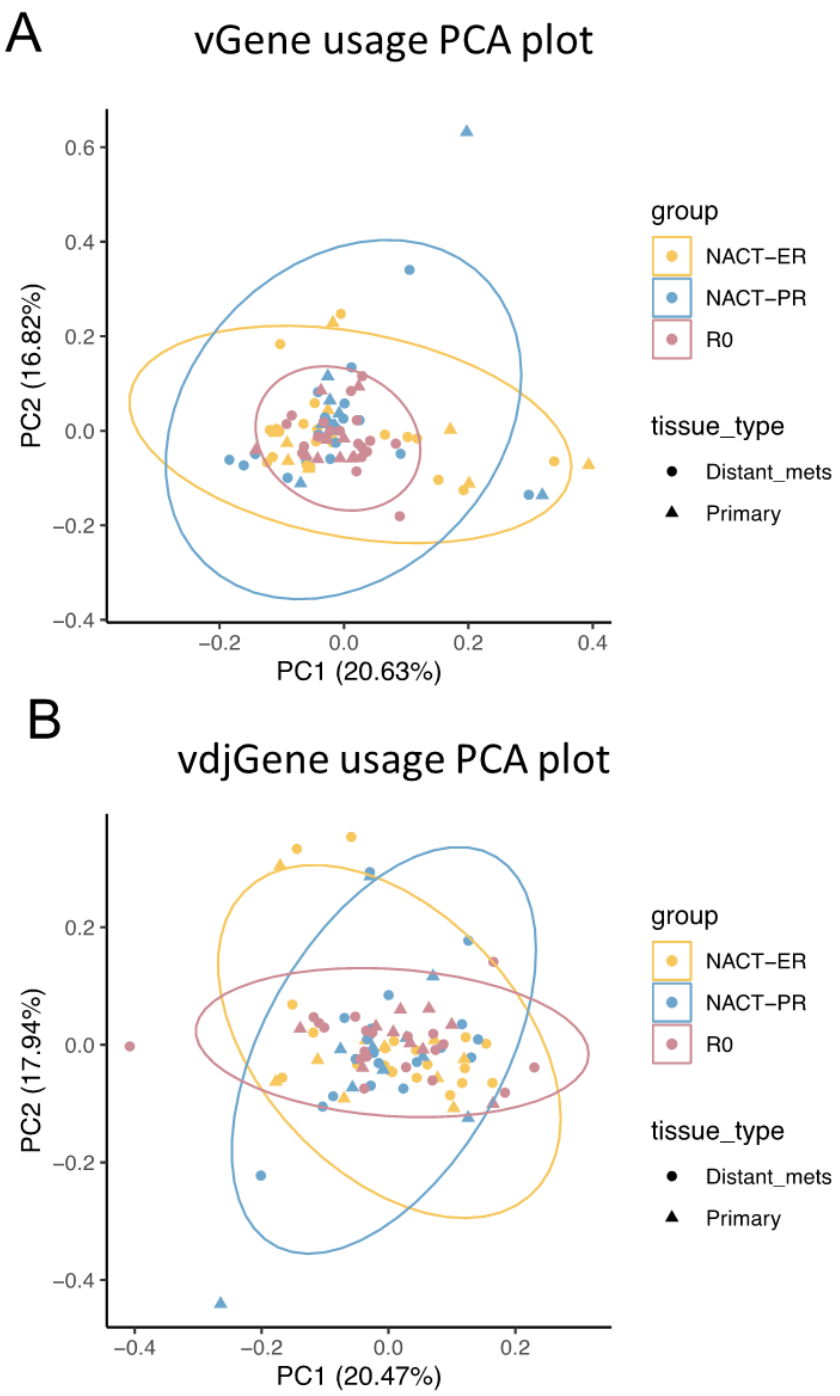

Figure S12. Principal component analysis of V gene usage (A) and V, D, and J gene usage (B) in the R0, NACT-ER, and NACT-PR groups, Related to Figure 4.

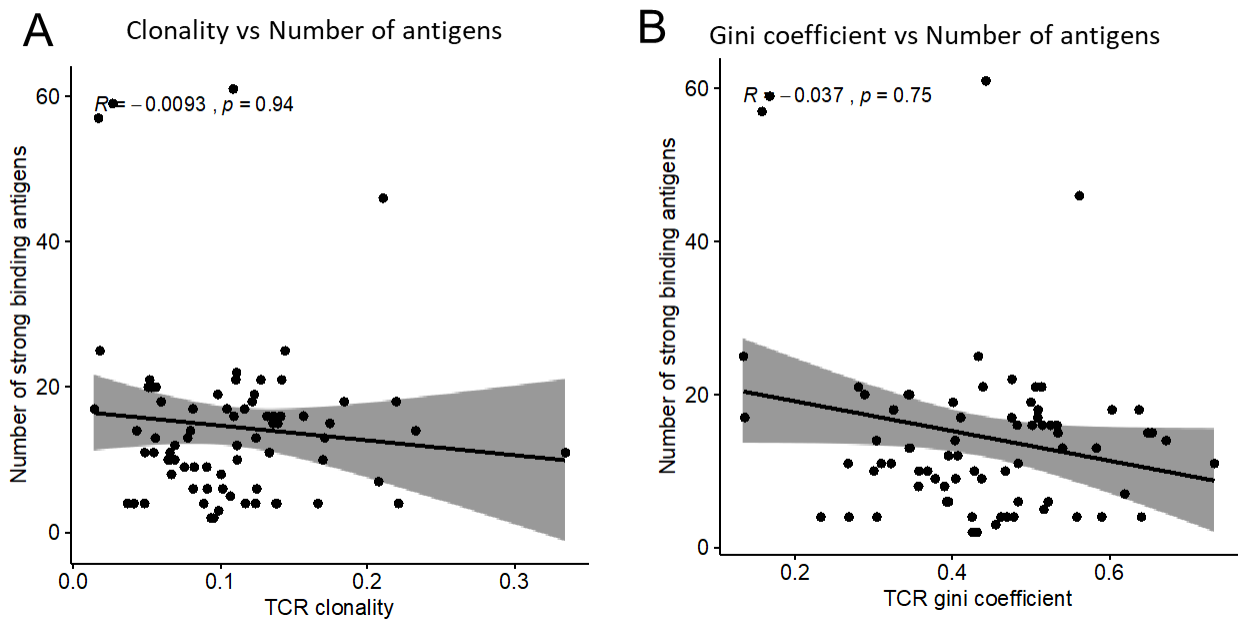

Figure S13. Correlation between TCR clonal diversity and level of strong-binding neoantigens, Related to Figure 5. (**A**) Correlations between TCR clonality and neoantigen level. (**B**) Correlation between TCR clonal evenness (Gini coefficient) and neoantigen level. The level of neoantigens was based on previous whole genome sequencing data; the total number of samples in this analysis was 75.

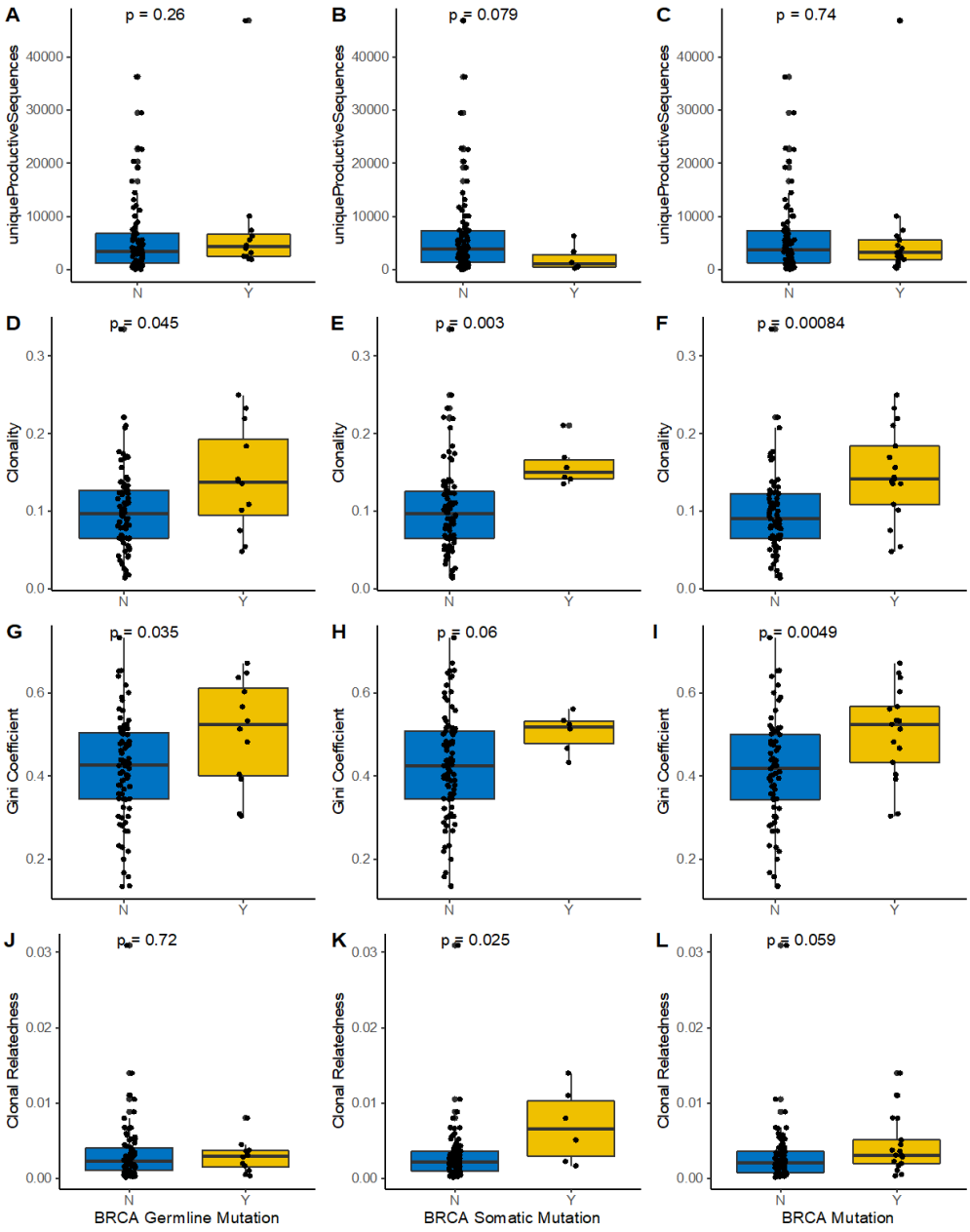

Figure S14. BRCA status and TCR diversity, Related to Figure 5. (A-C) Comparison of TCR richness between BRCA WT and BRCA mutant tumors including BRCA germline mutant (A), BRCA somatic mutant (B), and any BRCA mutant (germline or somatic) (C). **(D-F)** Comparison of clonality between BRCA WT and BRCA mutant tumors including BRCA germline mutant (D), BRCA somatic mutant (E), and any BRCA mutant (germline or somatic) (F). **(G-I)** Comparison of TCR evenness between BRCA WT and BRCA mutant tumors including BRCA germline mutant (G), BRCA somatic mutant (H), and any BRCA mutant (germline or somatic) (I). **(J-L)** Comparison of clonal relatedness between BRCA WT and BRCA mutant tumors including BRCA germline mutant (J), BRCA somatic mutant (K), and any BRCA mutant (germline or somatic) (L).

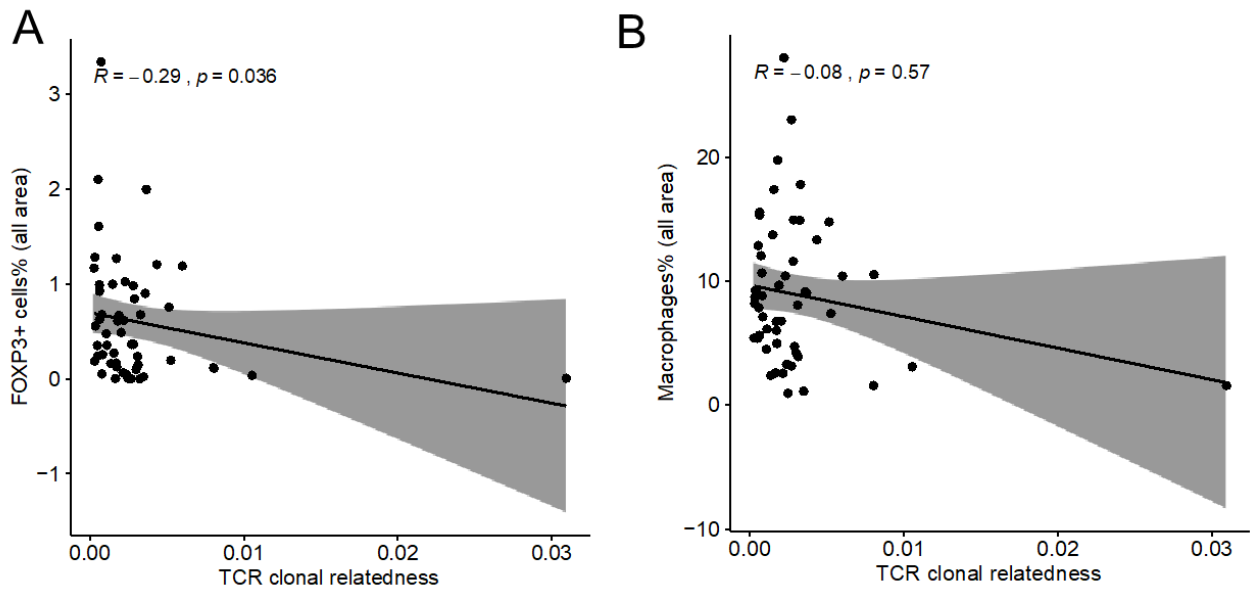

Figure S15. Correlation between immune cell percentage in all areas and TCR clonal relatedness, Related to Figure 5. (**A**) Correlation between the percentage of FOXP3+ cells and TCR clonal relatedness. (**B**) Correlation between the percentage of macrophage cells and TCR clonal relatedness. The percentage of certain immune cells was based on previous immune profiling data and included both the tumor and non-tumor areas. The total number of samples in this analysis was 53.

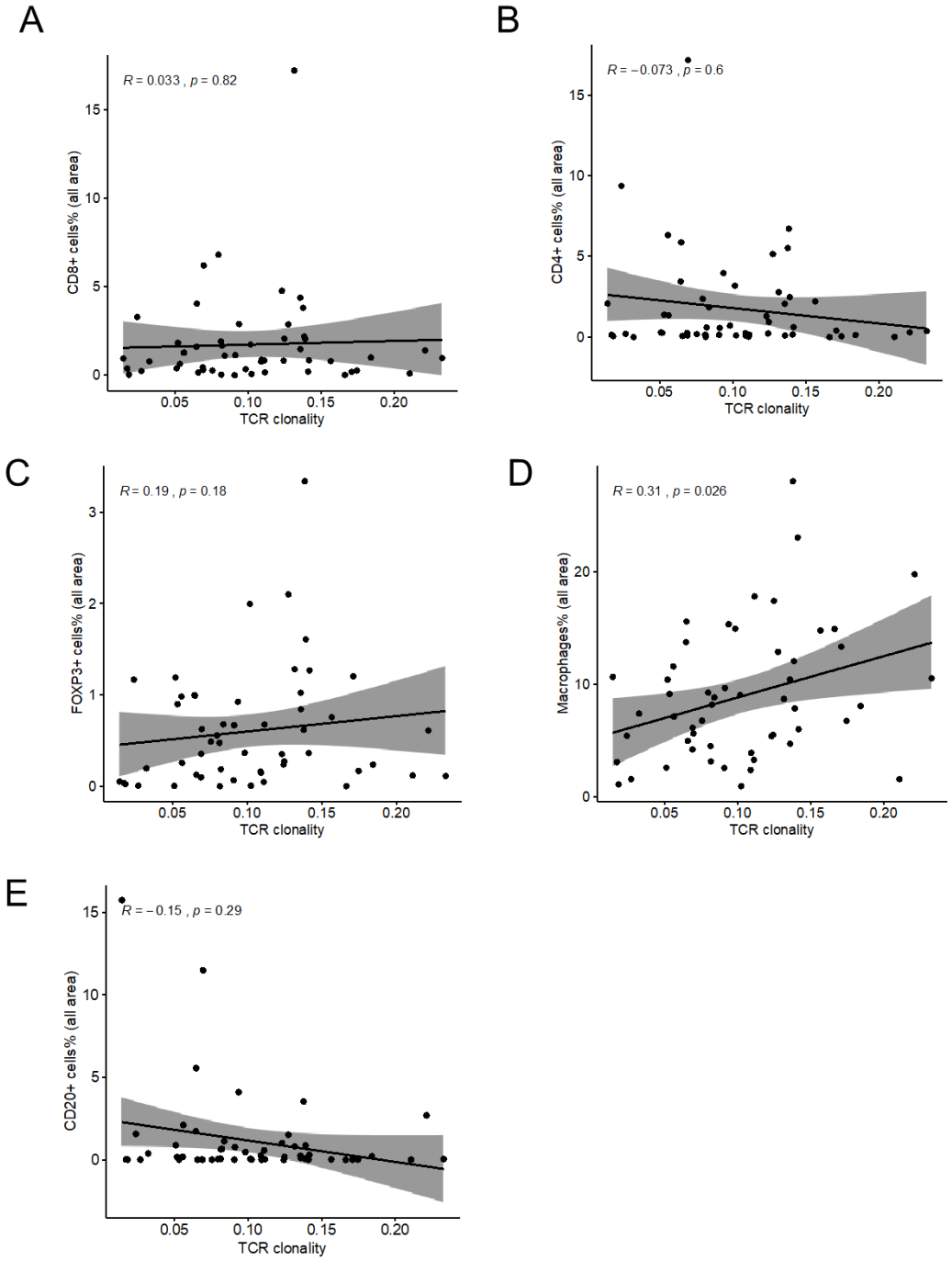

Figure S16. Correlation between immune cell percentages in all areas and TCR clonality, Related to Figure 5. (**A**) Correlation between the percentage of $CD8^+$ cells and TCR clonality. (**B**) Correlation between the percentage of $CD4^+$ cells and TCR clonality. (**C**) Correlation between the percentage of $FOXP3^+$ cells and TCR clonality. (**D**) Correlation between the percentage of macrophages and TCR clonality. (**E**) Correlation between the percentage of CD20+ cells and TCR clonality. The percentage of certain immune cells was based on previous immune profiling data and included both tumor and non-tumor areas. The total number of samples in this analysis was 53.

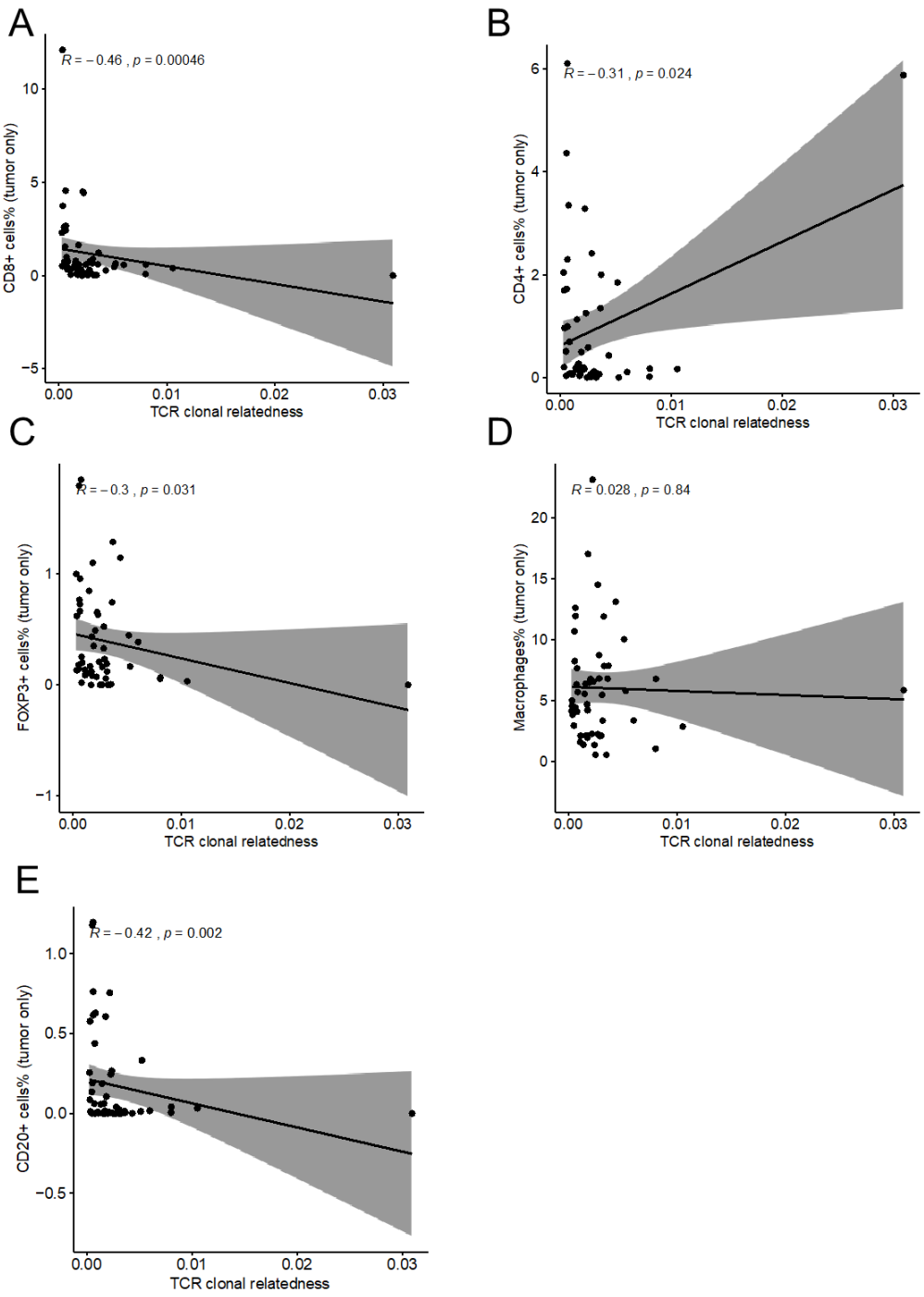

Figure S17. Correlation between immune cell percentages in tumor areas and TCR clonal relatedness, Related to Figure 5. (**A**) Correlation between the percentage of CD8$^+$ cells and TCR clonal relatedness. (**B**) Correlation between the percentage of CD4$^+$ cells and TCR clonal relatedness. (**C**) Correlation between the percentage of FOXP3$^+$ cells and TCR clonal relatedness. (**D**) Correlation between the percentage of macrophages and TCR clonal relatedness. (**E**) Correlation between the percentage of CD20+ cells and TCR clonal relatedness. The percentage of certain immune cells was based on previous immune profiling data and only included tumor areas. The total number of samples in this analysis was 53.

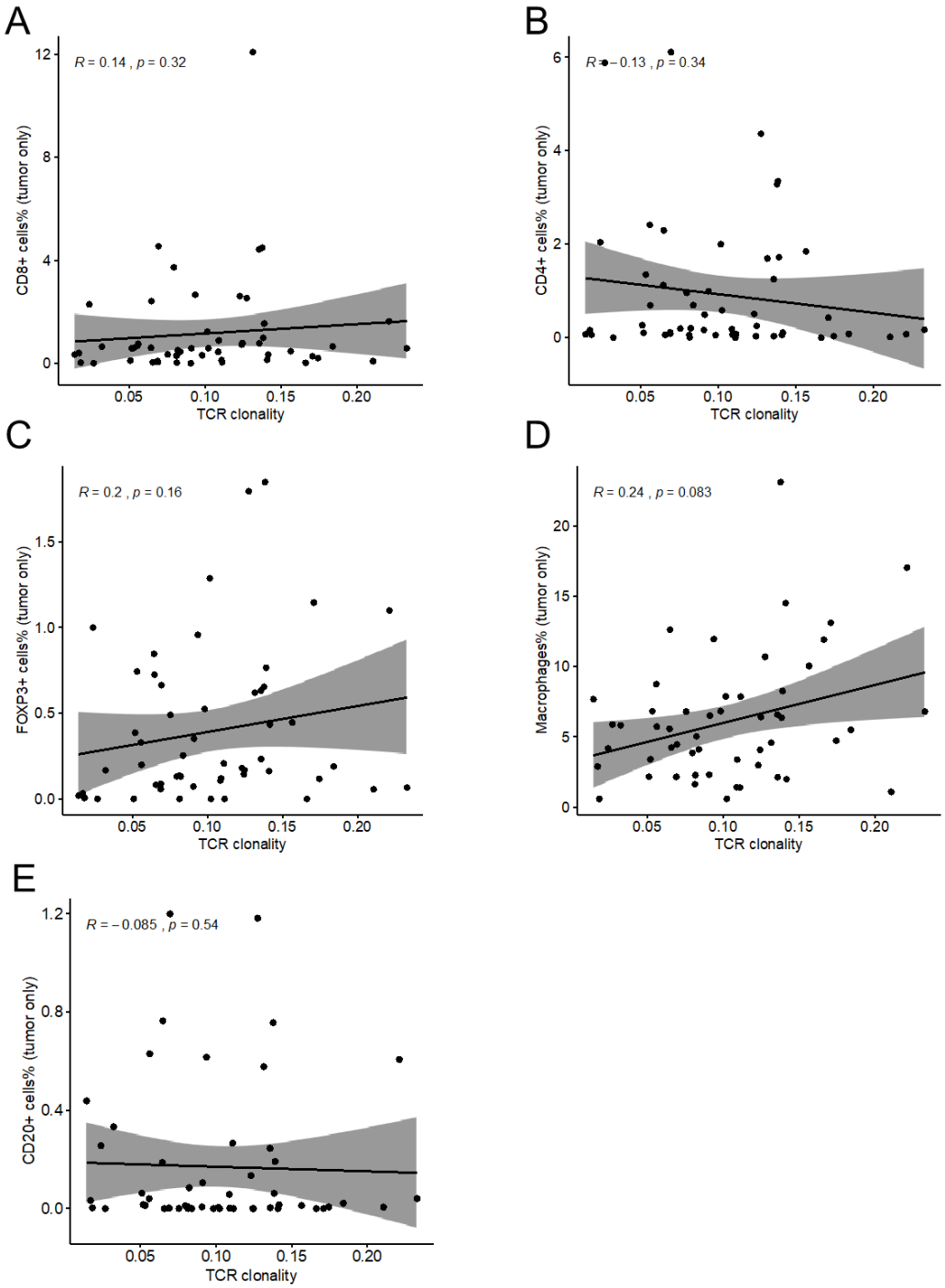

Figure S18. Correlation between immune cell percentages in tumor areas and TCR clonality, Related to Figure 5. (**A**) Correlation between the percentage of $CD8^+$ cells and TCR clonality. (**B**) Correlation between the percentage of $CD4^+$ cells and TCR clonality. (**C**) Correlation between the percentage of $FOXP3^+$ cells and TCR clonality. (**D**) Correlation between the percentage of macrophages and TCR clonality. (**E**) Correlation between the percentage of CD20+ cells and TCR clonality. The percentage of certain immune cells was based on previous immune profiling data and only included tumor areas. The total number of samples in this analysis was 53.

TRANSPARENT METHODS

Patients sample collection

Tissue samples were collected from 30 patients at The University of Texas MD Anderson Cancer Center (Houston, TX) Gynecologic Tumor Bank after obtaining written informed consent under an approved protocol by the Institutional Review Board, as we previously described (Lee et al., 2020). In brief, fresh-frozen tumor biopsy samples were collected from patients with HGSC managed under a systematic surgical algorithm (Fleming et al., 2018): complete gross resection after primary surgery (R0, n=10); poor tumor response to NACT with carboplatin and paclitaxel (NACT-PR, n=10); excellent tumor response to NACT (NACT-ER, n=10) (**Table S1**). According to the Response Evaluation Criteria in Solid Tumors (RECIST 1.1), response to NACT was considered poor if patients had stable or progressive disease after 3-4 cycles upon radiology evaluation and/or suboptimal interval cytoreduction after NACT. Besides, we considered excellent response if there was a complete response or only microscopic disease left at the time of interval surgery and/or pathology from interval surgery, as we previously described (Lee et al., 2020). One primary and two metastatic tumor samples were obtained from each patient before treatment and subjected to TCR sequencing.

Genomic DNA preparation

Genomic DNA samples from the 90 frozen tumor tissue samples were prepared by the Biospecimen Extraction Resource at MD Anderson, as we previously described (Lee et al., 2020). In brief, genomic DNA was extracted using the QIAamp DNA Mini Kit (QIAGEN), following the manufacturer's instructions. Extracted genomic DNA was

accurately quantified using Quant-iT PicoGreen dsDNA reagent and kit with a Qubit 3.0 Fluorometer (Invitrogen).

Human TCRβ sequencing

TCRβ sequencing was performed on genomic DNA that had been purified from tumor tissues using the Adaptive Biotechnologies immunoSEQ human TCRβ kit, following the manufacturer's instructions. Libraries were prepared using multiplex PCR primers that target the CDR3 of the human TCRβ gene after rearrangement of the V, D, and J gene segments. In brief, genomic DNA was accurately re-quantified using the Quant-iT PicoGreen dsDNA assay kit (Thermofisher) with a Qubit 3.0 Fluorometer (Invitrogen); quality was assessed using a 2200 TapeStation system (Agilent) following the manufacturer's instructions.

We split 400 ng of genomic DNA from each sample into two replicates for the first PCR set-up. We used the QIAGEN Multiplex PCR Kit (Qiagen); 31 cycles of the first PCR was used to amplify the highly variable CD3 region using V and J gene specific primers. Universal adapters at the end of V and J gene-specific primers served as targets for the addition of unique DNA barcodes in the second PCR. The amplicons were then purified using a bead based-system to remove residual primers and unamplified targets and were run on an agarose gel to confirm that the correct products were amplified. For the second PCR, the barcodes that were selected in the sample manifest and Illumina adapters were added to each PCR replicate during the 8 cycle second PCR. The libraries were then purified using a bead-based system that is similar to that used in first PCR to remove residual primers and unamplified targets. Another agarose gel check was performed to confirm whether the barcodes and Illumina adapters were added during the second PCR.

Equal volume of sequencing ready libraries were then pooled and run on an Agilent D1000 ScreenTape system (Agilent) to determine the size and size-adjusted concentration.

Using the Applied Biosystems QuantStudio 6 (Thermofisher) and KAPA Library Quantification kit (Roche), we quantified the libraries prior to sequencing. On the basis of the qPCR results, we loaded approximately 15 pM of the pooled libraries onto the MiSeq Sequencing System (Illumina) for a single end read, which included a 156-cycle Read 1 and a 15-cycle Index 1 read run. Raw sequences from the MiSeq were transferred to Adaptive's immunoSEQ Data Assistant, where the data were processed to determine the normalized and annotated TCRB repertoire profile of each sample. The data were then posted to the immunoSEQ Analyzer account to evaluate the immunosequencing data.

TCR sequencing analyses

The Bhattacharyya coefficient was used to determine the closeness of each of the two samples. It ranges from 0 to 1, where 0 means that there is no overlap at all and 1 means the TCR sequences and their frequencies are identical.

Clonality is derived from the Shannon entropy. The normalized Shannon entropy is calculated as Pielou's evenness (Kirsch et al., 2015), and the clonality score is defined as 1- (normalized entropy), as shown in Equation 1:

$$1 + \frac{\sum_i^N P_i log_2(P_i)}{log_2(N)} \qquad \text{(Equation 1)}$$

where p_i is the frequency of the TCR productive sequence *i* and *N* is the total number of unique productive sequences. The evenness was calculated by the Gini coefficient, which captures the inequality; it is defined as the area between the line of perfect equality (45-

degree line) and the observed Lorenz curve to the area between the line of perfect equality and the line of perfect inequality. Both the clonality and evenness score are measured on a scale from 0 to 1, where 0 indicates that all productive sequences have the same frequencies and 1 indicates that the repertoire is dominated by one single sequence.

Clonal relatedness is the fraction of unique nucleotide sequences that are related to the most frequent sequence by a defined edit distance threshold. The edit distance quantifies the similarity of two sequences by counting the minimum number of operations that are required to transform one sequence into the other; the edit distance threshold was set to be 10 in the analysis. Clonal relatedness considers both unproductive and productive sequences; the value ranges from 0 to 1, where 0 indicates that no sequences are related and 1 indicates that all sequences are related to the most frequent one.

TCR convergence refers to TCRs that are different on the nucleotide level but identical on the amino acid level. The TCR convergence score is calculated as the aggregate frequency of unique TCR nucleotide sequences that share the same variable gene and CDR3 amino acid sequence with at least one other clone in the sample.

The V, D and J genes and the overall CDR3 region were identified for each TCR sequence. The CDR3 length distribution was calculated and compared with the normal distribution. The Shapiro-Wilk test was used to test the normality of the observed CDR3 length distribution in each group. The V, D and J gene counts and frequencies were evaluated in each sample and compared across groups. Correlation among the V, D and J gene frequencies was calculated to determine the possibility of co-occurrence and

mutual exclusivity. The significance cut-off was $p< 0.01$. A principal component analysis was used to assess the overall variation of V, D, and J gene usage in different groups.

Integrative analyses

In the integrative analyses, the neoantigen level in each sample was determined from the whole genome sequencing data, as described in our previous work (Lee et al., 2020). The number of samples with both TCR sequencing and neoantigen results was 75. The percentages of various immune cells in the tumor area and all other areas were based on our previous immune profiling data (Lee et al., 2020); the number of samples with both TCR sequencing and immune profiling data was 53. Spearman correlation test was used to quantify the correlation between TCR clonal diversity and neoantigen levels, as well as the percentage of various immune cells.

Statistical analysis

All of the statistical analyses and plots were generated using R 4.0. As not all TCR variables met the normality assumption, the Wilcoxon signed-rank test (two-sided) was used to assess differences among groups; a p value <0.05 was used as the cut-off for significance. A Pearson correlation test was used to quantify the correlation among V, D, and J gene usage among patients in each group; a cut-off of p value <0.01 was used to assess significance. In the integrative analysis, the Spearman's rank correlation test was used to quantify the correlation between TCR clonal diversity and neoantigen levels, as well as the percentage of various immune cells. The significant positive or negative correlation was determined with a cut-off of Spearman Coefficient $R\leq-0.3$ or $R \geq 0.3$ and a p-value <0.01.

SUPPLEMENTAL REFERENCES

Kirsch, I., Vignali, M., and Robins, H. (2015). T-cell receptor profiling in cancer. Mol Oncol *9*, 2063-2070.

Lee, S., Zhao, L., Rojas, C., Bateman, N.W., Yao, H., Lara, O.D., Celestino, J., Morgan, M.B., Nguyen, T.V., Conrads, K.A.*, et al.* (2020). Molecular Analysis of Clinically Defined Subsets of High-Grade Serous Ovarian Cancer. Cell Rep *31*, 107502.